of melt veins in Acfer 040 probably began at a pressure and temperature in excess of 26 GPa and 2000°C. The presence of ilmenite demonstrates that shock-induced melt veins in chondrites continue to provide natural examples of important high-pressure minerals.

REFERENCES AND NOTES

1. E. A. Ringwood, *Composition and Petrology of the Earth's Mantle* (McGraw-Hill International Series in the Earth and Planetary Sciences, McGraw-Hill, New York, 1975), and references therein concerning synthesis of high-pressure minerals.
2. J. J. Gurney, *Diamonds in Kimberlites and Related Rocks*, vol. 2, *Geol. Soc. Am. Spec. Publ. 14, Proc. 4th Int. Kimberlite Conf.* (Blackwell, Oxford, 1989), p. 935.
3. R. A. Binns, R. J. Davis, S. J. B. Reed, *Nature* **221**, 943 (1969).
4. B. Mason, J. Nelen, J. S. White, *Science* **160**, 66 (1968).
5. J. V. Smith and B. Mason, *ibid.* **168**, 832 (1970).
6. A. Putnis and G. D. Price, *Nature* **280**, 217 (1979).
7. M. Chen and A. El Goresy, *Meteoritics* **29**, 456 (1994).
8. C. M. Lingemann and D. Stöffler, *ibid.* **29**, 491 (1994); *Lunar Planet. Sci.* **XXVI**, 851 (1995).
9. F. Langenhorst, P. Joreau, J.-C. Doukhan, *Geochim. Cosmochim. Acta* **59**, 1835 (1995).
10. M. Chen, T. G. Sharp, A. El Goresy, B. Wopenka, X. Xie, *Science* **271**, 1570 (1996).
11. C. M. Lingemann, F. Langenhorst, D. Stöffler, *Meteoritics* **30**, 537 (1995).
12. L.-G. Liu, *Geophys. Res. Lett.* **1**, 277 (1974).
13. N. Kawai, M. Tachimori, E. Ito, *Proc. Japan Acad.* **50**, 378 (1974).
14. L.-G. Liu, *Earth Planet. Sci. Lett.* **31**, 200 (1976).
15. M. Chen, T. G. Sharp, A. El Goresy, B. Wopenka, X. Xie, *Lunar Planet. Sci.* **XXVII**, 211 (1996); M. Chen, B. Wopenka, A. El Goresy, T. G. Sharp, *Meteoritics* **31**, A27 (1996).
16. T. G. Sharp, M. Chen, A. El Goresy, *Lunar Planet. Sci.* **XXVII**, 1175 (1996); *Meteoritics* **31**, A127 (1996).
17. A. Bischoff and T. Geiger, *Meteoritics* **30**, 113 (1995).
18. D. Stöffler, K. Keil, E. R. D. Scott, *Geochim. Cosmochim. Acta* **55**, 3845 (1991).
19. Polished thin sections of 20 μm thickness were used for optical, SEM, and microprobe investigations. Selected regions were then removed and prepared for TEM by ion-bombardment thinning. In order to minimize the damage to unstable compounds that can occur from heating and ion bombardment, the samples were prepared without the use of thermal adhesives, and ion milling was done using a liquid-nitrogen-cooled specimen holder. The low-temperature sample-preparation techniques were applied to samples studied in Bayreuth as well as selected samples studied previously in Münster. TEM was performed using Philips CM20 and CM20-FEG instruments operated at 200 kV, and both instruments were equipped with Noran Voyager analytical systems for energy-dispersive x-ray spectroscopy (EDS).
20. G. L. Nord Jr. and C. A. Lawson, *Am. Mineral.* **74**, 160 (1989).
21. P. E. Champness and G. W. Lorimer, *J. Mat. Sci.* **8**, 467 (1973); G. W. Lorimer and P. E. Champness, *Am. Mineral.* **58**, 243 (1973); G. L. Nord Jr., J. S. Huebner, M. Ross, *Lunar Planet. Sci.* **VIII**, 732 (1977); G. L. Nord Jr., *Phys. Chem. Miner.* **6**, 109 (1980).
22. S. Heinemann, T. G. Sharp, F. Seifert, D. C. Rubie, *Phys. Chem. Miner.* **24**, 206 (1997).
23. D. Hugh-Jones, T. Sharp, R. Angel, A. Woodland, *Eur. J. Mineral.* **8**, 1337 (1996); D. A. Hugh-Jones and R. J. Angel, *Am. Mineral.* **79**, 405 (1994); D. A. Hugh-Jones, A. B. Woodland, R. J. Angel, *ibid.* **79**, 1032 (1994).
24. T. Irifune, *Nature* **370**, 131 (1994).
25. Y. Wang, F. Guyot, R. Liebermann, *J. Geophys. Res.* **97**, 12327 (1992).
26. C. M. McCammon, D. C. Rubie, C. R. Ross II, F. Seifert, H. St. C. O'Neill, *Am. Mineral.* **77**, 894 (1992).
27. H. Mori, *J. Mineral. Soc. Japan* **23**, 171 (1994).
28. C. B. Agee, *Nature* **346**, 834 (1990); C. B. Agee, J. Li, M. C. Shannon, S. Ciercone, *J. Geophys. Res.* **100**, 17725 (1995).
29. T. Irifune, T. Koizumi, J.-I. Ando, *Phys. Earth Planet. Inter.* **96**, 147 (1996).
30. S. E. Kesson, J. D. FitzGerald, J. M. G. Shelley, *Nature* **372**, 767 (1994).
31. J. Zhang and C. Herzberg, *J. Geophys. Res.* **99**, 17729 (1994).
32. T. Gasparik, *ibid.* **97**, 15181 (1992).
33. M. J. Toplis, G. Libourel, M. R. Carrol, *Geochim. Cosmochim. Acta* **58**, 797 (1994).
34. M. Chen, B. Wopenka, A. El Goresy, T. G. Sharp, *Meteoritics* **29**, 98 (1996).
35. T. G. Sharp, M. Chen, A. El Goresy, *Lunar Planet. Sci.* **XXVIII**, 1283 (1997).

36. We thank two anonymous reviewers for helpful suggestions in the improvement of the manuscript. This work is part of a Ph.D. thesis (C.M.L.) at the Institut für Planetologie, Westfälische Wilhelms-Universität, Münster. It was partially supported by the Deutsche Forschungsgemeinschaft (DFG).

11 March 1997; accepted 19 June 1997

The Ionosphere of Europa from Galileo Radio Occultations

A. J. Kliore,* D. P. Hinson, F. M. Flasar, A. F. Nagy, T. E. Cravens

The Galileo spacecraft performed six radio occultation observations of Jupiter's Galilean satellite Europa during its tour of the jovian system. In five of the six instances, these occultations revealed the presence of a tenuous ionosphere on Europa, with an average maximum electron density of nearly 10^4 per cubic centimeter near the surface and a plasma scale height of about 240 ± 40 kilometers from the surface to 300 kilometers and of 440 ± 60 kilometers above 300 kilometers. Such an ionosphere could be produced by solar photoionization and jovian magnetospheric particle impact in an atmosphere having a surface density of about 10^8 electrons per cubic centimeter. If this atmosphere is composed primarily of O_2, then the principal ion is O_2^+ and the neutral atmosphere temperature implied by the 240-kilometer scale height is about 600 kelvin. If it is composed of H_2O, the principal ion is H_3O^+ and the neutral temperature is about 340 kelvin. In either case, these temperatures are much higher than those observed on Europa's surface, and an external heating source from the jovian magnetosphere is required.

The Galileo spacecraft is in orbit about Jupiter, studying Jupiter and the Galilean satellites (Io, Europa, Ganymede, and Callisto). Of these, only Io was known to have an atmosphere, which was observed by a radio occultation (*1*) of Pioneer 10 in 1973 (*2*). Observations and theoretical considerations suggest that Europa may have an atmosphere that originates from frozen surface water ice, most likely produced by particle impact (*3*, *4*). Therefore, any atmosphere must consist of some mixture of H_2O, H, H_2, OH, O_2, and O. Early Pioneer 10 observations suggested an atomic oxygen column density of around 1×10^{13} cm^{-2} (*5*), but these measurements may have been contaminated. Recent Hubble Space Telescope (HST) observations of the 1304–1356 Å lines of atomic oxygen were used to deduce an O_2 column density of about 1.5×10^{15} cm^{-2} (*6*). Recent Galileo measurements at Ganymede and Callisto indicated the presence of atomic hydrogen, with densities on the order of 1×10^4 cm^{-3} (*7*), which might suggest similar abundances at Europa.

A search for an atmosphere on Europa was carried out when Galileo was occulted by Europa three times: on 19 December 1996 (E4) and on 20 and 25 February 1997 (E6a and E6b). The parameters defining the properties of these occultations are given in Table 1. For a few minutes before and after the occultations, the S band (2.295 GHz, or about 13 cm wavelength) radio signal from Galileo traversed regions above Europa's surface in which one could observe the effects of refraction by an atmosphere, or more precisely, an ionosphere (a layer of ions and electrons produced in tenuous regions of the atmosphere by photoionization and magnetospheric particle impact), should one exist on Europa. Thus, the three occul-

A. J. Kliore, Jet Propulsion Laboratory, California Institute of Technology, Pasadena, CA 91109, USA.
D. P. Hinson, Center for Radar Astronomy, Stanford University, Stanford, CA 94305, USA.
F. M. Flasar, Laboratory for Extraterrestrial Physics, NASA/Goddard Space Flight Center, Greenbelt, MD 20771, USA.
A. F. Nagy, Space Physics Research Laboratory, University of Michigan, Ann Arbor, MI 48109, USA.
T. E. Cravens, Department of Physics and Astronomy, University of Kansas, Lawrence, KS 66045, USA.

*To whom correspondence should be addressed.

tations provided six opportunities to search for Europa's ionosphere. It was necessary to use the low-gain antenna to transmit the signal from Galileo, as the high-gain antenna failed to deploy properly. This meant that the signal level received by the Deep Space Net (DSN) stations at Canberra, Australia (E4), and Goldstone, California (E6a and E6b), was reduced by a factor of almost 1000 (30 dB). Also, only one frequency, S band, could be used rather than two coherently related frequencies at S band and X band (8.415 GHz, or 3.56-cm wavelength). The resulting signal-to-noise ratio, even when the 70-m-diameter antennas of the DSN were used, was on the order of 14 dB in a 1-Hz bandwidth. Five of the six occultation measurements were conducted in the one-way mode, with the downlink frequency referenced to the on-board ultrastable oscillator (USO) (8) having a stability of about one part in 10^{12}, except for the E6a entry, which was done in the two-way mode in which the frequency transmitted by Galileo is referenced to a frequency standard at the DSN station.

The received signals were translated in frequency down to an audio frequency range, filtered in a bandpass of 0 to 2500 Hz, and digitized to 8-bit samples at a rate of 5000 samples per second. The digital data were processed with a digital phase-locked loop program analyzing 1-s data blocks to obtain time series of the frequency and signal strength. Removing the programmable local oscillator (PLO) (9) "steering function" results in a time series of "sky frequency," which is what one would have observed without a PLO. This time series was compared to a time series of predicted frequency computed from a precise spacecraft ephemeris, and their difference forms the frequency residuals, which are the basic data used in determining the profiles of electron density above the surface of Europa. Ideally, these residuals should have a zero mean on the baseline, which is the portion of the data that is away from the influence of possible ionospheric refraction effects. In reality, because of drift in the USO, effects of the long propagation path through the interplanetary medium, and imperfect knowledge of the frequency transmitted by Galileo and of the spacecraft trajectory, this baseline has not only a nonzero mean but also a slope, which over periods of tens of minutes can be approximated by a linear frequency drift. The bias and linear drift in the residuals were removed by fitting of a straight line to the baseline data. When this was done, the baseline was seen to contain many frequency oscillations, some of a magnitude similar to that of the frequency deviations that occurred when the radio link was near the surface and presumably were caused by propagation through Europa's ionosphere. When the fitted residuals were integrated with respect to time to produce phase residuals, a number of linear features that abruptly changed back and forth from positive to negative slopes were observed. These linear features were clearly not random but were caused by abrupt positive and negative frequency steps on the order of a few millihertz, which probably are caused by gradients in the interplanetary plasma between the spacecraft and Earth. These frequency steps were computed from the magnitude and duration of the linear phase features and were removed throughout each data set. This procedure reduced the peak-to-peak excursions of the residual phase on the baseline by about a factor of 10, making the final results far less dependent on where on the baseline the linear function fit is applied. This step is crucial to the analysis, because the maximum frequency excursions, presumably due to a Europa ionosphere, are only on the order of 20 to 40 mHz.

The corrected residuals were then converted to refraction angle by application of the Europa-centered trajectory information derived from the Galileo navigation ephemeris, with iterative corrections for light propagation time between the spacecraft and the limb of Europa and from the limb to the DSN stations. These data were then inverted with the use of well-known techniques (*10–12*) to obtain the refractivity, or $(n - 1) \times 10^6$, as a function of altitude. This is directly related to the electron density through a constant that is dependent on the inverse square of the frequency. The geometry of each measurement is illustrated in Table 1. The occultation locations, which are depicted by the diagrams in Figs. 1 through 3, are widely different because each occultation occurred when Europa was in a different place in its orbit about Jupiter. All occultations occurred within about 5° of the terminator.

The electron density profiles show the presence of ionization in the Europa atmosphere in five of the six measurements. The observation when no ionosphere was detected—E6a exit (Fig. 2)—occurred at a ram angle of nearly 180°, near the middle of the wake region, where the electron density could be expected to be depleted. In contrast, the observations during the E4 occultation (Fig. 1) were made at ram angles close to 90°, where the line of sight lay along the wake direction, thus perhaps enhancing the electron density and giving rise to effects caused by the absence of spherical symmetry. The maximum electron densities in the other cases ranged from about 6×10^3 cm^{-3} to about 11×10^3 cm^{-3} and occurred at or near the surface of Europa. There are significant differences between individual mea-

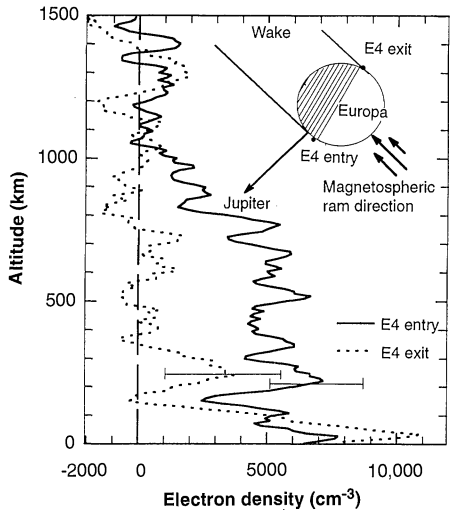

Fig. 1. The E4 occultation of Galileo by Europa. The locations of the occultation points relative to the magnetospheric ram direction and the terminator are shown by the inset diagram. The error bars in Figs. 1 through 3 represent three times the standard deviation of the baseline data computed from the altitude of the first data point down to 1000 km. The apparent enhancement of ionization up to about 500 km in the entry observation may be an effect of looking along the wake direction.

Table 1. Geometry of the Galileo occultations by Europa, listing the date, distance from the limb, latitude, longitude, solar zenith angle (SZA), and the magnetospheric ram angle. The ram angle is defined as the angle between the vector pointing from the center of Europa to the "sub-ram" point and the one pointing from the center to the occultation point. Because all occultations occurred at near-equatorial latitudes, this angle can be approximated by the difference in longitude between the occultation point and 270°, which is the sub-ram longitude.

Observation	Date	Distance (km)	Latitude (degrees)	W longitude (degrees)	SZA (degrees)	Ram angle (degrees)
E4 entry	19 Dec.1996	1,600	−2	346	95	76
E4 exit	19 Dec.1996	4,000	−4	167	85	103
E6a entry	20 Feb.1997	1,500	−24	281	86	11
E6a exit	20 Feb.1997	4,400	−21	102	94	168
E6b entry	25 Feb.1997	2,777,500	−14	56	85	146
E6b exit	25 Feb.1997	2,776,700	−14	236	95	34

surements, so for the purpose of modeling, an average electron density profile was computed, which is shown in Fig. 4. The average electron density has a maximum of about $9 \times 10^3 \pm 4 \times 10^3$ cm^{-3} and a plasma scale height of about 240 ± 40 km below 300-km altitude and about 440 ± 60 km above 300-km altitude. These electron densities may be the result of photoionization, impact ionization, or a combination of both. The various likely scenarios and the resulting implications for the presence of an atmosphere around Europa are discussed in the following paragraphs.

First we consider the case of an ionosphere with an electron density of 1×10^4 cm^{-3} near the surface. The photoabsorption cross sections at extreme ultraviolet (EUV) wavelengths of H_2O, O_2, O, H_2, OH, and H, which are the likely neutral atmospheric constituents, are not very different; a value of $\sim 3 \times 10^{-17}$ cm^2 is a reasonable approximation. Therefore, if the ionosphere is in a region where the optical depth is less than unity, the column density above the surface needs to be less than $\sim 3 \times 10^{16}$ cm^{-2}. If the atmospheric scale height is ~20 km (*4*), then the surface density has to be less than 1.5×10^{10} cm^{-3} in order to ensure an optical depth of less than unity. An upper limit on the column density of $\sim 3 \times 10^{15}$ cm^{-2} was also suggested by Johnson (*3*). He argued that the atmosphere is created by slow (~100 eV) ion sputtering of the surface, then these ions must be able to reach the surface, thus setting an upper limit on the column density. The HST observations (*6*) suggest that an atmosphere consisting primarily of O_2 should be considered first, under the assumption that chemical processes dominate at the altitude region of maximum electron density. Assuming dissociative recombination as the dominant loss process for the O_2^+ ions, the neutral density required to produce an electron density of n_e at zero optical depth is $[O_2] = n_e^2 \alpha/\xi$, where α is the dissociative recombination rate and ξ is the ionization frequency. Taking the terrestrial photoionization frequency of about 9×10^{-7} s^{-1} (*13*) adjusted for Jupiter distance ($\sim 3.3 \times 10^{-8}$ s^{-1}), a recombination rate constant of 1×10^{-7} cm^3 s^{-1}, and an electron density of 1×10^4 cm^{-3}, one gets an O_2 density of $\sim 3 \times 10^8$ cm^{-3}. This required density is reduced if additional ionization due to electron impact is considered. Schreier *et al.* (*14*) used measured plasma parameters from Voyager and estimated a total electron impact ionization rate of 1.88×10^{-7} s^{-1}. This ionization rate is more than a factor of 5 larger than the rate for photoionization and thus leads to a required molecular oxygen density that is smaller, namely $\sim 5 \times 10^7$ cm^{-3}.

If the major neutral constituent is not O_2 but one of the other likely candidate constituents such as H_2O, H, H_2, OH, and O, the atmospheric density requirement does not change very much. Any of the other three molecular candidates will not change the above requirement significantly, because neither the dissociative recombination rate coefficients nor the ionization frequencies are significantly different. For example, if H_2O is taken to be the dominant neutral molecular species, which leads to H_3O^+ as the main ion species, the required neutral density is still on the order of 10^8 cm^{-3}. If the neutral atmosphere consists of a mixture of atomic and molecular species, the conclusion is very similar, because both H^+ and O^+ can charge-exchange rapidly with one of the molecular neutral species, forming molecular ions.

The measured electron density scale height is on the order of 240 km in the lowest 300 km, which implies a neutral gas scale height of 120 km in a region where chemical processes dominate. This neutral scale height corresponds to a gas temperature of about 340 K for H_2O and 610 K for O_2. These temperatures are significantly higher than the apparent surface temperature of about 130 K (*15*); therefore, they require further consideration. A first-order estimate of the energy required, as an energy inflow at the top of the atmosphere, to maintain this elevated atmospheric temperature is on the order of 10^{10} eV cm^{-2} s^{-1}, which is more than a factor of 100 less than that which could be obtained from the surrounding jovian magnetosphere. This does not necessarily imply the presence of such a heat source, but it is energetically well within the realm of possibility. We also note that the upper limit of the solar column heating rate at Europa is about 1×10^9 eV cm^{-2} s^{-1}.

Next, let us look at the issue of optical depth and column density in light of the atmospheric density values that have just been obtained. If the larger number density requirement is imposed, corresponding to photoionization (3×10^8 cm^{-3}), col-

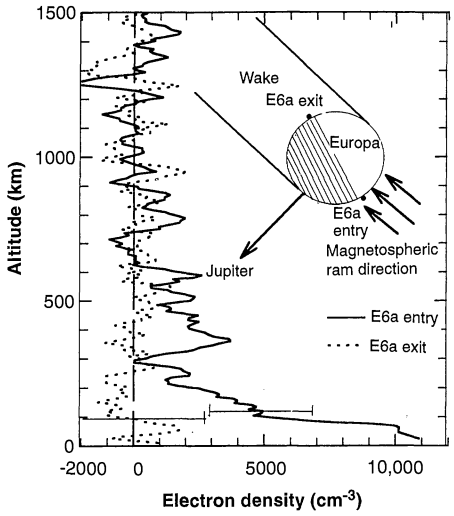

Fig. 2. The E6a occultation. The lack of an observable ionosphere in the exit observation is most probably due to its location, which is almost in the middle of the anti–ram wake region, which may be depleted of ionization.

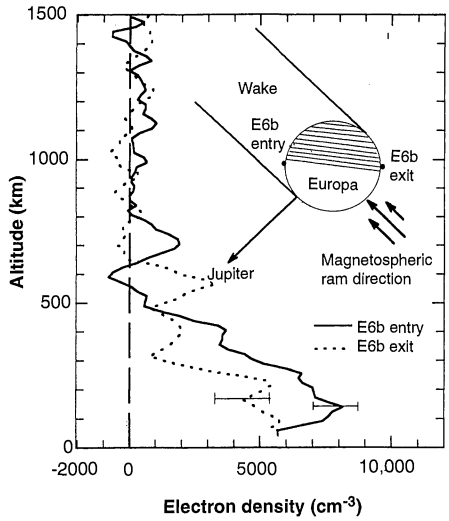

Fig. 3. The E6b occultation. The similarity of the entry and exit observations is puzzling, because the former lies on the ram side and the latter lies well within the wake region.

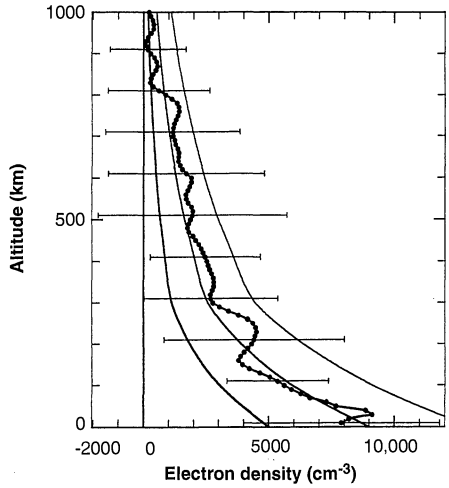

Fig. 4. Average electron density profile computed from the five observations in which an ionosphere was detected. The error bars represent the square root of the sum of the squares of the standard deviation of the mean and the standard deviations of the data along the baseline of each data set. The average profile (line with dots) is best described by a model having a plasma scale height of 240 ± 40 km below 300 km and 440 ± 60 km above that altitude (smooth solid lines).

umn densities of about 6×10^{14} cm^{-2} and 3.6×10^{15} cm^{-2} are obtained for assumed neutral atmosphere scale heights of 20 and 120 km, respectively. Even the larger column density, if reduced by the factor of 5 corresponding to additional electron impact ionization, brings the required column density below the value set by Hall *et al.* (6). It should also be pointed out that these column densities do lead to an optical depth of less than unity, which was assumed at the beginning of this discussion. It is now appropriate to address the validity of the assumption of chemical equilibrium conditions. The chemical time constant near the surface (~500 s), given the observed scale height, is significantly smaller than the diffusive time constant (~10^4 s); thus, the assumption is a good one.

The near-surface atmospheric densities and temperatures that were found to be consistent with the ionospheric observations, namely a number density of ~10^8 cm^{-3} and a temperature of ~340 to 600 K, correspond to a surface pressure of 0.01 nbar. This value is comparable to about the limit set by the Voyager UV spectrometer for Ganymede (*16*), but no comparable limits are available for Europa.

A very unlikely scenario would lead to a density requirement that is significantly lower than any discussed here so far. This is the case of an atmosphere that consists solely of atomic hydrogen or oxygen, with no molecular species being present. The required atmospheric density is very different in this case, because the loss of atomic ions by either radiative recombination, corresponding to a lifetime of about 10^7 s, or diffusion to the surface, with a lifetime of about 10^6 s, are both very slow processes. In this scenario, transport processes related to Europa's interaction with Jupiter's magnetosphere are likely to be most important.

Finally, it should be pointed out that the external magnetospheric thermal plasma and magnetic pressures on Europa's ionosphere are about 2×10^{-8} and 2×10^{-7} Nm^{-2}, respectively. Even if the electron and ion temperatures are allowed to be four times greater than the neutral gas temperature, the peak ionospheric thermal plasma pressure, calculated with the measured peak electron density, is still significantly less than the external one. This means that the ionosphere will be strongly magnetized and coupled to the magnetosphere.

REFERENCES AND NOTES

1. Radio occultations, in which a spacecraft appears to go behind a planetary body as viewed from Earth, allow the spacecraft-Earth radio link to traverse the ionosphere and atmosphere of the occulting body. Interpretation of the effects on the phase and amplitude of the signal received on Earth of refraction and defocusing in the planetary atmosphere and ionosphere allows one to infer the electron density structure in the ionosphere and the temperature-pressure profiles and absorption characteristics of the neutral atmosphere. This technique has been used with much success to measure the characteristics of the ionospheres and atmospheres of Venus, Mars, Jupiter, Saturn, Uranus, and Neptune, as well as Saturn's satellite Titan, Neptune's Triton, and Jupiter's Io and now Europa (*12*).
2. A. J. Kliore, D. L. Cain, G. Fjeldbo, B. L. Seidel, S. I. Rasool, *Science* **183**, 323 (1974).
3. R. E. Johnson, *Energetic Charged-Particle Interactions with Atmospheres and Surfaces* (Springer Verlag, Berlin, 1990).
4. W. H. Ip, *Icarus* **120**, 317 (1996).
5. F. M. Wu, D. L. Judge, R. W. Carlson, *Astrophys. J.* **325**, 325 (1978).
6. D. T. Hall, D. F. Strobel, P. D. Feldman, M. A. McGrath, H. A.Weaver, *Nature* **373**, 677 (1995).
7. C. Barth *et al.*, *Geophys. Res Lett.*, in press; C. Barth, personal communication.
8. H. T. Howard *et al.*, *Space. Sci. Rev.* **60**, 565 (1992).
9. The PLO is used to steer the center frequency of the receiver bandwidth in accordance with a predicted function based on the spacecraft trajectory.
10. G. Fjeldbo, A. J. Kliore, V. R. Eshleman, *Astron. J.* **76**, 123 (1971).
11. A. J. Kliore, in *NASA TM X-62,150*, L. Colin, Ed. (NASA/Ames Research Center, Mountain View, CA, 1972).
12. G. F. Lindal, *Astron. J.* **103**, 967 (1992).
13. M. R. Torr and D. G. Torr, *J. Geophys. Res.* **90**, 6675 (1985).
14. R. Schreier, A. Eviatar, V. M. Vasyliunas, J. D. Richardson, *ibid.* **98**, 21231 (1993).
15. W. M. Calvin, R. N. Clark, R. H. Brown, J. R. Spencer, *ibid.* **100**, 19041 (1995).
16. L. Broadfoot *et al.*, *Science* **204**, 979 (1979); S. Kumar and D. M. Hunten, in *Satellites of Jupiter*, D. Morrison, Ed. (Univ. of Arizona Press, Tucson, AZ, 1982), pp. 782–806.

17. We wish to acknowledge the contributions of the staff of the Galileo Project, who have carried out a highly successful mission under difficult circumstances; the Galileo Navigation team, with W. E. Kirhofer and J. Johannesen, without whose precise orbits this work would not have been possible; and the personnel of the Jet Propulsion Laboratory Multimission Radio Science team, especially S. Asmar, R. Herrera, D. Chong, P. Eshe, P. Priest, J. Caetta, T. Rebold, and S. Abbate, who planned and successfully executed the data acquisition process. Special thanks are due to J. Twicken and P. Schinder for their assistance in data analysis at Stanford and Goddard Space Flight Center, and to D. M. Hunten, W. H. Ip, and two anonymous referees for helpful suggestions and comments. This work was supported by NASA contracts and grants.

28 April 1997; accepted 17 June 1997

Experimental Simulations of Sulfide Formation in the Solar Nebula

Dante S. Lauretta,* Katharina Lodders, Bruce Fegley Jr.

Sulfurization of meteoritic metal in H_2S-H_2 gas produced three different sulfides: monosulfide solid solution [$(Fe,Ni)_{1-x}S$], pentlandite [$(Fe,Ni)_{9-x}S_8$], and a phosphorus-rich sulfide. The composition of the remnant metal was unchanged. These results are contrary to theoretical predictions that sulfide formation in the solar nebula produced troilite (FeS) and enriched the remaining metal in nickel. The experimental sulfides are chemically and morphologically similar to sulfide grains in the matrix of the Alais (class CI) carbonaceous chondrite, suggesting that these meteoritic sulfides may be condensates from the solar nebula.

Chondrites are the most primitive meteorites and may contain condensates that could serve as probes of the solar nebula environment. Unfortunately, even the most primitive meteorites experienced some degree of secondary processing—such as aqueous alteration, thermal metamorphism, or impact shock—that transformed nebular condensates into secondary phases. Therefore, criteria to distinguish pristine nebular condensates from secondary alteration products in chondrites are required. Experimental simulations of the gas-solid reactions that formed nebular minerals are one method to determine such criteria.

Planetary Chemistry Laboratory, Department of Earth and Planetary Sciences, Campus Box 1169, Washington University, One Brookings Drive, St. Louis, MO 63130–4899, USA.

*To whom correspondence should be addressed. E-mail: lauretta@wunder.wustl.edu

Sulfide minerals are ubiquitous in chondrites. The most common sulfides in carbonaceous chondrites are pyrrhotite ($Fe_{1-x}S$) and pentlandite [$(Fe,Ni)_{9-x}S_8$] (*1*). Stoichiometric pyrrhotite is troilite (FeS), and Ni-bearing pyrrhotites are members of the monosulfide solid solution [mss, $(Fe,Ni)_{1-x}S$]. In addition, P-bearing sulfides were recently found in CM chondrites (*2*, *3*). Because the characteristics of nebular sulfides were poorly understood, we experimentally simulated their formation in the solar nebula to determine the resulting mineralogy, morphology, and composition (*4*). By characterizing nebular sulfides in this manner, we can determine which, if any, of the sulfides in carbonaceous chondrites are unaltered nebular condensates.

We formed an experimental metal-sulfide assemblage by heating a piece of the Canyon Diablo iron meteorite for 30 days